ELSEVIER

Applied Catalysis A: General 125 (1995) 271–291

APPLIED CATALYSIS A: GENERAL

# Kinetics of ethylbenzene hydrogenation on $Ni/Al_2O_3$

Stefan Smeds, Dmitry Murzin [1], Tapio Salmi *

*Laboratory of Industrial Chemistry, Åbo Akademi, Biskopsgatan 8, FIN-20500 Åbo, Finland*

Received 20 September 1994; revised 14 December 1994; accepted 14 December 1994

**Abstract**

The gas-phase hydrogenation kinetics of ethylbenzene on $Ni/Al_2O_3$ was investigated in a differential microreactor at atmospheric pressure and 130–190°C. Rapid deactivation of the catalyst complicated the steady-state measurements. Reaction orders were near zero for the aromatic compound and between 1.2 (130°C) and 2.3 (190°C) for hydrogen. A rate maximum was observed at 160–175°C, depending on the concentration ratio of the reactants. Mechanistic modelling suggested that the reaction rate is governed by three steps of pairwise sequential addition of hydrogen atoms to adsorbed ethylbenzene. The partially hydrogenated surface intermediates were proposed to have aromatic character. The physical reasonability of the model parameters was discussed.

*Keywords:* Ethylbenzene; Hydrogenation; Kinetics; Nickel; Reaction kinetics

## 1. Introduction

Despite the large amount of work done in investigating the hydrogenation of aromatics, no general agreement upon the reaction mechanism exists. This is of course partly caused by the different conditions used in the experiments (catalyst, temperatures, pressures), leading to different mechanistic explanations for the reaction kinetics.

Hydrogenation of ethylbenzene on nickel gives ethylcyclohexane as the main product:

* Corresponding author. E-mail tsalmi@abo.fi, Tel. (+358-21) 2654311, fax. (+358-21) 2654479.

[1] Permanent address: Karpov Institute of Physical Chemistry, Vorontsovo Pole 10, Moscow 103064, Russia.


*SSDI* 0926-860X(95)00002-X

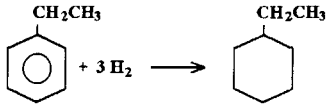


Investigations of ethylbenzene hydrogenation are very sparse and mainly restricted to comparisons of the hydrogenation rates of different alkylbenzenes. For instance, Völter et al. [1] included ethylbenzene in their study of activity and activation energies of gas-phase hydrogenation of alkylbenzenes on nickel.

A number of authors have reported on gas-phase hydrogenation of benzene on nickel. Van Meerten and Coenen [2] arrived at a mechanism where the surface addition steps (by single atoms) are determining the overall rate and have equal rate constants. Similar ideas had already been proposed by Snagovskii et al. [3]. Other authors have suggested that hydrogen is added in the form of molecules [4,5] to the adsorbed benzene molecule. Mirodatos et al. [5] proposed, based on isotopic transient studies, that the addition of hydrogen is in fact occurring pairwise to benzene on nickel at low temperature and low hydrogen pressure. Different views also exist concerning whether the coadsorption of benzene and hydrogen is competitive [5] or non-competitive [2]. Reaction of hydrogen directly from the gas phase with adsorbed benzene has been proposed by Kehoe and Butt [6].

Gas-phase hydrogenation of toluene on nickel has been investigated more sparsely [7–9]. Klvana et al. [7] observed zero-order dependence towards both compounds and suggested interaction between strongly adsorbed toluene and hydrogen on separate sites as the rate determining step. Mamaladze et al. [8] proposed slow formation of a reactive complex involving three physically adsorbed hydrogen molecules, and fast consecutive isomerization to methylcyclohexane. Recently, Lindfors and Salmi [9] suggested addition of hydrogen atom pairs to adsorbed toluene as rate determining steps, toluene and hydrogen being adsorbed competitively.

The aim of this work is to investigate systematically the kinetics of ethylbenzene hydrogenation in the gas phase on $Ni/Al_2O_3$ at wide ranges of temperatures and pressures. Comparison with previously presented kinetics and mechanisms of benzene and toluene hydrogenation might give new insight on the mechanism of hydrogenation of the aromatic ring.

## 2. Experimental

The kinetic steady-state experiments were performed in a laboratory-scale differential reactor (glass, 3 mm diameter) using helium as an inert diluent. A commercial 17 wt.-% $Ni/Al_2O_3$ catalyst (Engelhard, sample mass 30 mg, BET area 104 $m^2/g$, particle size 0.15 mm) was used, keeping the conversion generally below 4% (at most around 10%). Hydrogen ( > 99.5%) and helium ( > 99.9995%)

from AGA were further purified by passing the gases through an ML Oxy-Filter (Cu catalyst) and an ML 5 Å molecular sieve for oxygen trapping. Ethylbenzene (anhydrous >99%) obtained from Aldrich was used as received.

Before the experiments the catalyst was reduced in flowing hydrogen (200 ml/min) for 2 h at 500°C. Regeneration of a used catalyst to re-establish its initial activity was carried out in flowing hydrogen (200 ml/min) for 2 h at 400°C. Heating and cooling of the catalyst was always conducted at a rate of 200°C/h to avoid structural changes. The reactant and product concentrations were monitored on-line using an isothermally operating Varian gas chromatograph (GC) equipped with a flame ionization detector and a fused silica column.

Varian Star Chromatography Workstation software was used to monitor and process the GC signal, whereas Microsoft Visual Basic in connection with a DT2801 data translation card on a personal computer was used to make the laboratory procedures (re-activation and kinetic measurement) semi-automatic. A HP 5790 GC-MS was used for qualitative analysis of the condensed product flow.

The temperature of the kinetic experiments was 130°C–190°C (15°C intervals). The ethylbenzene partial pressure was varied from 0.1 bar to 0.35 bar, whereas the hydrogen partial pressure was kept in the range of 0.4–0.9 bar, giving 12 data points at each temperature. Including a few extra checks the total number of experimental observations was 71.

## 3. Results and discussion

### *3.1. Kinetic data*

The main hydrogenation product was ethylcyclohexane, however ethylcyclohexene was also detected in concentrations of around 1% of the main product concentration. Traces of toluene and $C_3$–$C_4$ alkylbenzenes as well as their hydrogenated products were detected by GC–MS. These components were proved not to originate from the inlet stream, and are therefore supposed to be formed through disproportionations in the substituent chain. The absence of heat and mass transfer limitations was checked according to literature criteria [10,11].

Considerable reversible deactivation was observed during the hydrogenation, decreasing the activity roughly by 20% during the first hour on stream for the mildest conditions (low aromatic partial pressures). For the more severe conditions (high aromatic partial pressures) the activity decreased dramatically to a minor fraction of the initial activity during the same initial time period. The activity for the first hour on stream for some of the experimental conditions is shown in Fig. 1. Deposition of some hydrogen-deficient species on the surface is the probable cause for this reversible deactivation [12]. The initial activity could always be completely restored by regenerating the catalyst for 2 h at 400°C in flowing hydrogen. This reversibility in the presence of hydrogen disallowed measurements of pure hydro-

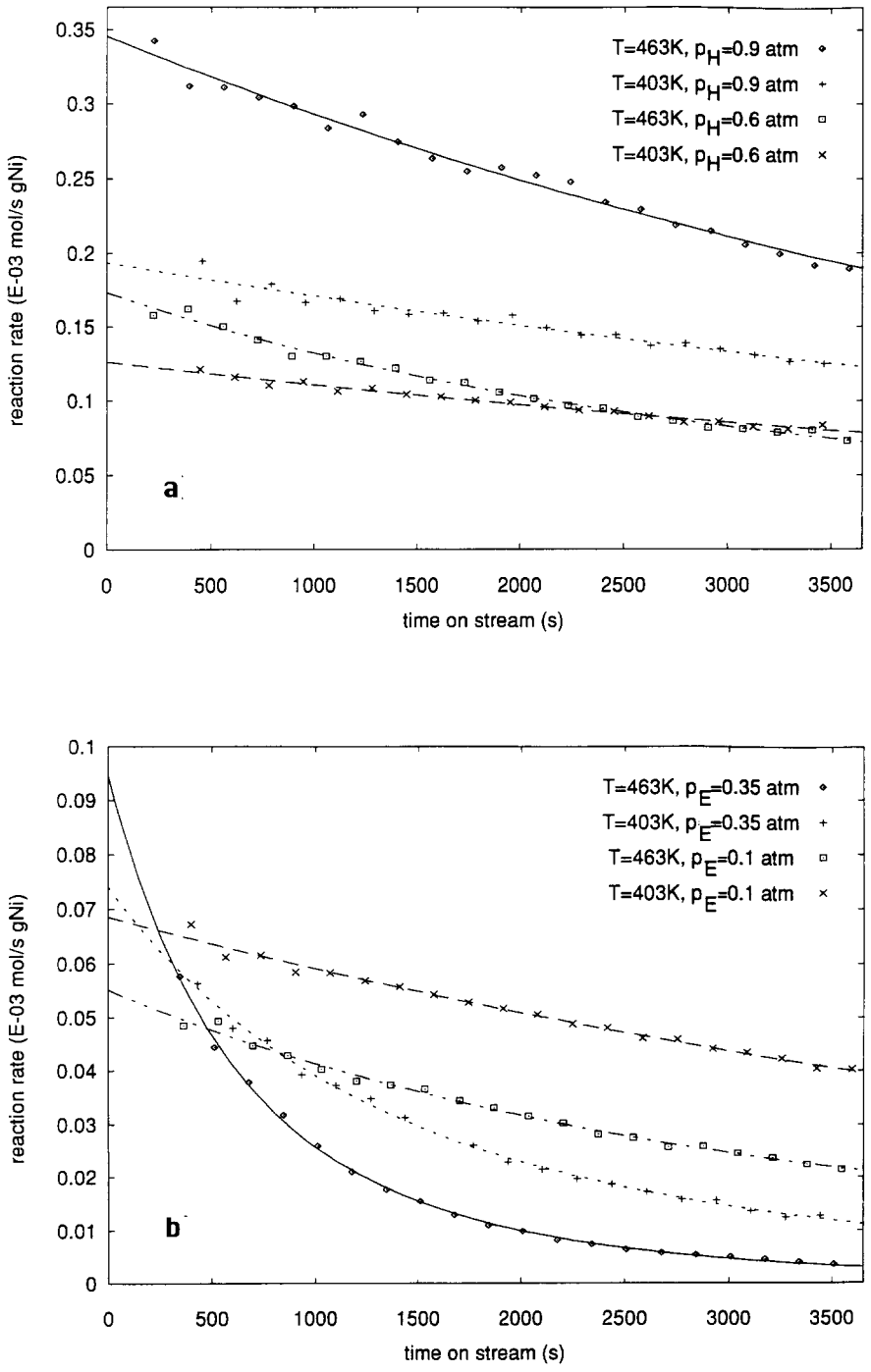


Fig. 1. Catalyst activity during the first hour on stream (a): $p_E = 0.1$ bar (b): $p_H = 0.4$ bar.

genation kinetics on an aged catalyst sample, since changing the concentration of hydrogen in the reactor would alter the activity level of the catalyst. Chou and Vannice [13] solved this problem on palladium by including the dehydrogenation of the aromatic compound (benzene) to hydrogen-deficient species in the kinetic model. However, small differences in the activity level still exist, depending on different conditions of the preceding measurements [13].

To exclude any influence of different sample history, an extrapolation procedure to initial activity according to the empirical equation [14]

$$r(t) = \frac{r_0}{(1+at)^b} \tag{1}$$

was adopted in this work. Here $r_0$ is the steady-state rate at time zero and will be referred to as initial rate, $a$ and $b$ are empirical constants and $t$ is time. This procedure necessitates reactivation of the catalyst sample immediately before every single kinetic measurement. The fit of Eq. (1) to some of the steady-state measurements is also shown in Fig. 1. As can be seen from the figure, the predicted rates follow closely the experimental rates.

The irreversible changes in the catalyst activity were below 20% during a series of more than 30 experiments with subsequent regenerations of the same catalyst sample. To take this into account every eighth experiment on average was a repeated deactivation (irreversible) check experiment and the level of the initial activity was normalized according to these irreversible deactivation tests. The standard deviation of six subsequent deactivation tests was calculated to 2.3%. This figure can, however, only be regarded as a rough estimate of the standard deviation of experiments, since the (modelled) deactivation behaviour is different for different conditions. Detailed mechanistic modelling of the deactivation kinetics would prompt for more knowledge of the surface chemistry involved. This is, however, not within the scope of the present paper.

The dependence of the initial rate on temperature is shown in Fig. 2. A rate maximum was observed around 160°C–175°C, depending on the partial pressures of the reactants. This temperature rate maximum is consistent with earlier studies of gas-phase hydrogenation of aromatic compounds [2,4,5,8,9,13]. The initial rate dependence on the hydrogen pressure is shown in Fig. 3. At low temperature (130°C) the apparent reaction order for hydrogen is about 1.2, increasing to about 2.3 at the highest temperature (190°C). Fig. 4 describes the initial rate dependence on the partial pressure of ethylbenzene (E). The observed reaction order for ethylbenzene increases from near zero at low temperatures to around 0.3 at high temperatures. To obtain a phenomenological description of the rate data, the extended power-law model [15]

$$r = \frac{k p_E^m p_H^n}{(1 + K_1 p_E + K_2 p_H)^l} \tag{2}$$

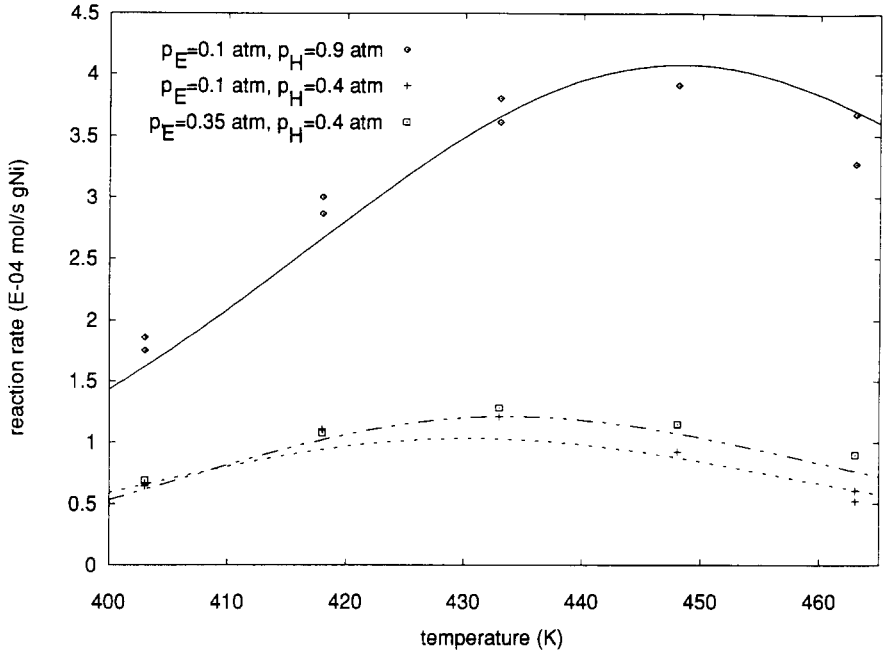


Fig. 2. Reaction rate as a function of temperature.

was fitted to the data ($p_E$ = ethylbenzene pressure, $p_H$ = hydrogen pressure). Table 1 gives the parameter values calculated with non-linear regression, taking the temperature dependence of $K_i$ ($bar^{-1}$) as that of an adsorption equilibrium constant:

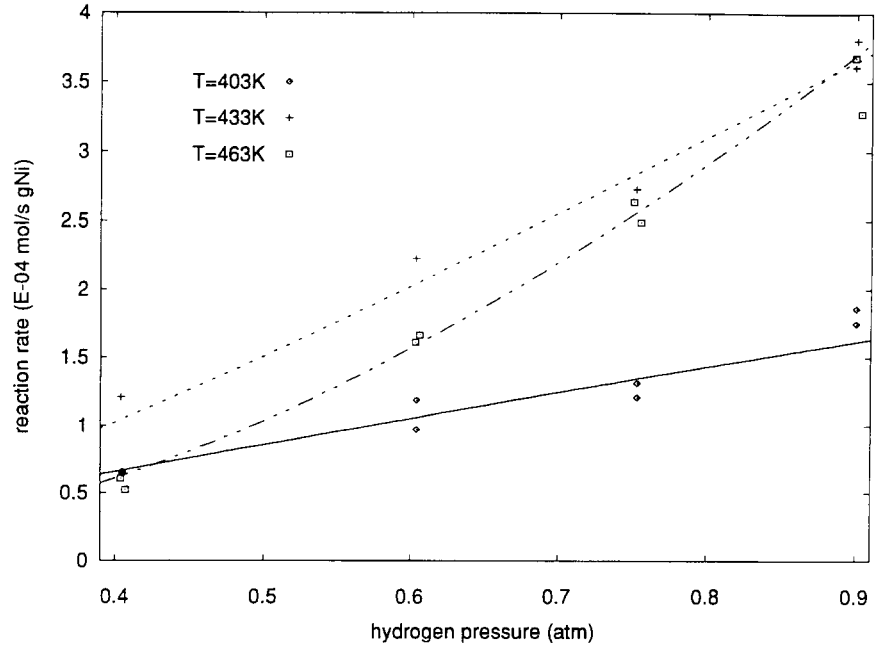


Fig. 3. Reaction rate as a function of hydrogen pressure.

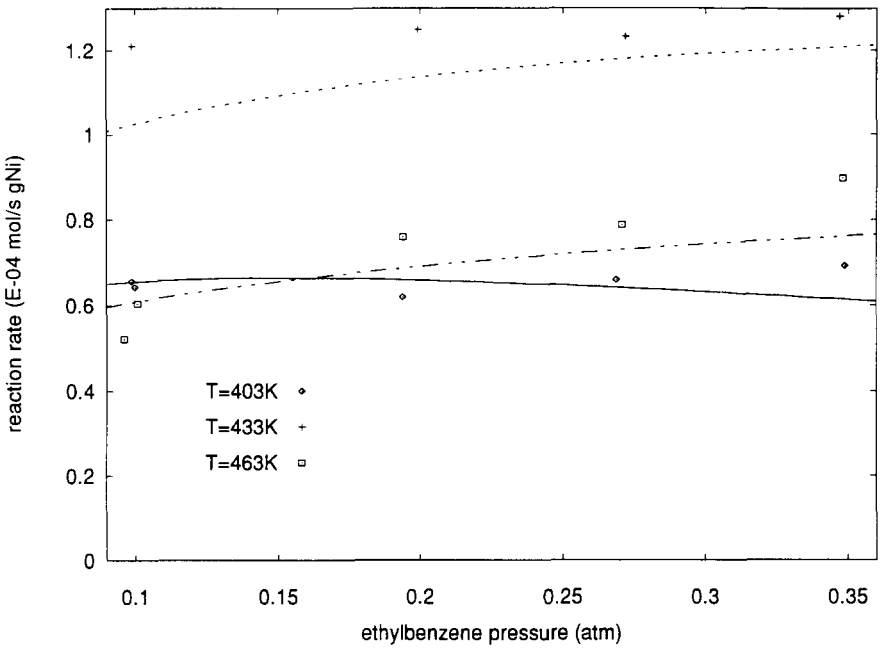


Fig. 4. Reaction rate as a function of ethylbenzene pressure.

$$K_i(T) = e^{\frac{\Delta S_i}{R}} e^{\frac{-\Delta H_i}{RT}} \tag{3}$$

where $\Delta S_i$ is adsorption entropy for species $i$ and $\Delta H_i$ is adsorption enthalpy for species $i$. The constants $k$ were assumed to obey the Arrhenius law in the form [16]

$$k(T) = k(\bar{T}) e^{\frac{-E}{RT'}} \tag{4}$$

where $\bar{T}$ is the average temperature of the experimental temperature region ($\bar{T}=433$ K) and T′ is given by

$$\frac{1}{T'} = \frac{1}{T} - \frac{1}{\bar{T}} \tag{5}$$

Table 1
Kinetic parameters (95% confidence), residual sum of squares (SSQ, arb. units) and mean residual sum of squares (MRSQ, arb. units) for the extended power-law rate model, $k_i = [\,] \cdot 10^{-4}$ mol s$^{-1}$ $g_{Ni}^{-1}$, $E_i = [\,] \cdot$ kJ mol$^{-1}$, $\Delta S_i = [\,] \cdot$ J mol$^{-1}$ K$^{-1}$, $\Delta H_i = [\,] \cdot$ kJ mol$^{-1}$

| | |
|---|---|
| *MRSQ* | 0.20 |
| *SSQ* | 12.5 |
| $m$ | $0.19 \pm 0.08$ |
| $n$ | $3.0 \pm 0.8$ |
| $l$ | $2.3 \pm 0.9$ |
| $k(\bar{T})$ | $170 \pm 390$ |
| $-E$ | $-94 \pm 48$ |
| $-\Delta S(K_1)$ | $290 \pm 180$ |
| $-\Delta H(K_1)$ | $120 \pm 73$ |
| $-\Delta S(K_2)$ | $150 \pm 37$ |
| $-\Delta H(K_2)$ | $68 \pm 16$ |

The model (2) can reproduce the temperature and partial pressure dependencies of the reaction studied (Figs. 2–4).

### 3.2. Kinetic modelling and data fitting

Since hydrogenation of ethylbenzene involves destruction of the aromatic ring as in benzene hydrogenation, we will refer to previous studies reported on benzene hydrogenation on other metals as well. Recently Chou and Vannice [13] presented a kinetic model for gas-phase benzene and toluene hydrogenation on palladium, featuring sequential addition of adsorbed hydrogen atoms to benzene molecules adsorbed on another type of sites, as well as concurrent formation of hydrogen-deficient surface species. Their results suggest weak hydrogen and benzene adsorption, the adsorbed species being mobile on the surface. The calculated values of the rate constants of the six rate determining surface addition steps were almost equal. This would imply that adsorbed cyclohexene as such cannot possibly be an intermediate surface species, since the hydrogenation rate of cyclohexene is several orders of magnitude higher than has been reported for benzene [17].

Due to our procedure of calculating initial rates it was reasonable to use only the hydrogenation part of the model of Chou and Vannice [13] for data fitting. The rate equation can be written as follows:

$$r = k_6 \left( \frac{(K_H p_H)^{0.5}}{1 + (K_H p_H)^{0.5}} \right) \left( \frac{Y_6 K_B p_B}{1 + K_B p_B (1 + Y_1 + Y_2 + Y_3 + Y_4 + Y_5)} \right) \quad (6)$$

where B denotes the aromatic molecule and $Y_1 \ldots Y_6$ are functions of the rate and adsorption constants, however too complex to be reproduced here [13]. The data fitting results are shown in Fig. 5 and the calculated parameter values are listed in Table 2. Fig. 5 shows that the overall description of the model is acceptable. Also no clear deviations from a random distribution of the residuals as functions of the independent variables ($T$, $p_H$, $p_B$) could be seen. The adsorption parameter values in Table 2 suggest weak hydrogen adsorption ($\Delta H_H \approx -20$ kJ mol$^{-1}$) and slightly mobile adsorbed species ($\Delta S_H \approx -110$ J mol$^{-1}$ K$^{-1}$, $\Delta S_E \approx -140$ J mol$^{-1}$ K$^{-1}$). For the surface rate constants a decreasing trend with the degree of hydrogen addition was obtained, the rate constant of the first step being two orders of magnitude greater than that of the last step. This is in contradiction with the view of ethylcyclohexadiene and ethylcyclohexene as surface intermediates, since higher rate constants would then be expected for the later addition steps.

The kinetic modelling of this work takes into account both competitive and non-competitive adsorption of the two reactants, dissociative and non-dissociative adsorption of hydrogen, as well as the possibility of several slow surface reaction steps. According to isotopic transient studies [5] hydrogen is added pairwise, either in the form of atoms or molecules. Adsorption steps were assumed to be in pseudo-equilibria, desorption of the reaction product was presumed to be fast and irrevers-

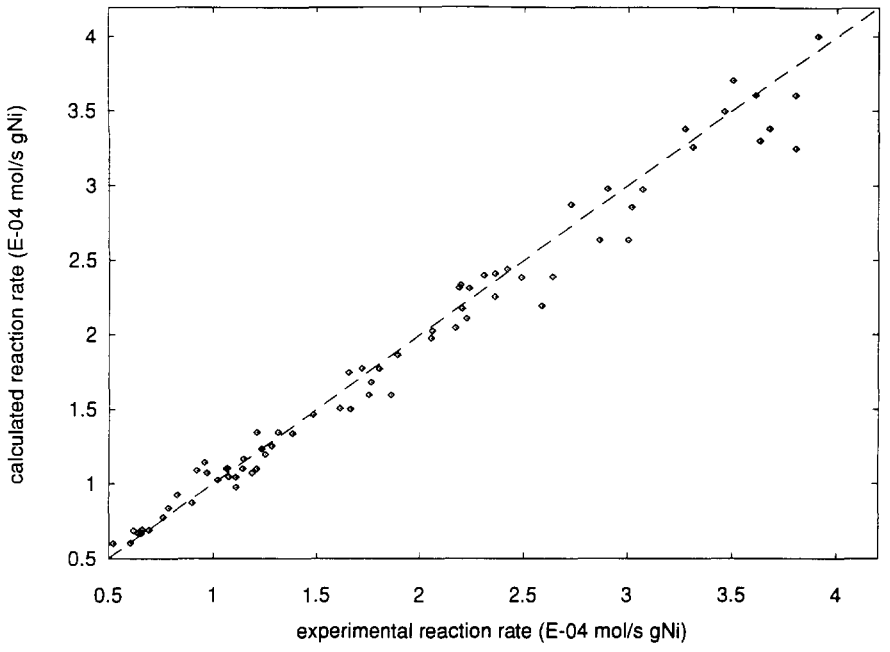


Fig. 5. Results of fit for the model of Chou and Vannice [13]: calculated versus experimental reaction rate.

ible. This irreversibility is justified, since the measured conversions were far from equilibrium conversions even at the highest temperature. The steps leading to deactivation were not included in the reaction mechanism due to the procedure of calculation of initial rates. Thus the initial steady-state rate data were fitted to pure hydrogenation reaction models.

The reaction mechanisms considered can be summarized according to the following scheme:

Table 2
Kinetic parameters, residual sum of squares (*SSQ*, arb. units) and mean residual sum of squares (*MRSQ*, arb. units) for the model of Chou and Vannice, using the notation of ref. [13], $k_i = [\,] \cdot 10^{-4}$ mol $s^{-1}$ $g_{Ni}^{-1}$, $E_i = [\,] \cdot$ kJ $mol^{-1}$, $\Delta S_i = [\,] \cdot$ J $mol^{-1}$ $K^{-1}$, $\Delta H_i = [\,] \cdot$ kJ $mol^{-1}$

| | |
|---|---|
| *MRSQ* | 0.19 |
| *SSQ* | 11.4 |
| $k_1(\bar{T})$ | 49 000[a] |
| $-E_1$ | 110[a] |
| $k_{-1}(\bar{T})$ | 1400[a] |
| $-E_{-1}$ | 89[a] |
| $k_6(\bar{T})$ | 980[a] |
| $-E_6$ | 50[a] |
| $k_{-6}(\bar{T})$ | 3.2[a] |
| $-E_{-6}$ | 110[a] |
| $-\Delta S_H$ | 110[a] |
| $-\Delta H_H$ | 20[a] |
| $-\Delta S_E$ | 140[a] |
| $-\Delta H_E$ | 70[a] |

[a] 95% confidence intervals could not be calculated due to coupling between the parameters.

$$H_2(g) + j^* \overset{K_H}{\rightleftharpoons} jH^*_{2/j}$$

$$E(g) + S \overset{K_A}{\rightleftharpoons} ES$$

$$ES + jH_{2/j}{}^* \underset{k_{-1}}{\overset{k_1}{\rightleftharpoons}} EH_2S + j^*$$

$$EH_2S + 2H_{2/j}{}^* \underset{k_{-2}}{\overset{k_2}{\rightleftharpoons}} EH_4S + j^*$$

$$EH_4S + 2H_{2/j}{}^* \overset{k_3}{\rightarrow} EH_6S + j^*$$

$$EH_6S \rightarrow EtCH + S$$

---

$$E + 3H_2 \rightarrow EtCH$$

where $^*$ denotes an active site for hydrogen (H), S is an active site for the aromatic compound (E), $j$ is either 1 (non-dissociative adsorption) or 2 (dissociative adsorption) and EtCH is ethylcyclohexane. It should be noted that for competitive adsorption S coincide with $X$ $^*$-sites, where $X$ is the number of $*$-sites occupied by ethylbenzene. The rates of the surface steps become:

$$r_1 = k_1\theta_E\theta_H^j - k_{-1}\theta_{EH_2}\theta_*^j \quad (7)$$

$$r_2 = k_2\theta_{EH_2}\theta_H^j - k_{-2}\theta_{EH_4}\theta_*^j \quad (8)$$

$$r_3 = k_3\theta_{EH_4}\theta_H^j \quad (9)$$

where $\theta_i$ denotes surface coverage of component $i$. Under steady-state conditions the rate of the three surface addition steps are equal:

$$r = r_1 = r_2 = r_3 \quad (10)$$

Quasi-equilibria for the adsorption steps of hydrogen and ethylbenzene give:

$$K_H = \frac{\theta_H^j}{p_H\theta_*^j} \quad (11)$$

$$K_E = \frac{\theta_E}{p_E\theta_S} \quad \text{non-competitive adsorption}$$

$$K_E = \frac{\theta_E}{p_E\theta_*^X} \quad \text{competitive adsorption} \quad (12)$$

The coverages of hydrogen and the partially hydrogenated intermediates can be expressed with the fraction of vacant sites and the coverage of ethylbenzene, using the relations (7)–(11):

$$r=\frac{k_3\frac{k_1}{k_{-1}}\frac{k_2}{k_{-2}}(K_H p_H)^3\theta_E\theta_*^j}{1+\frac{k_3}{k_{-2}}(K_H p_H)+\frac{k_2k_3}{k_{-1}k_{-2}}(K_H p_H)^2} \tag{13}$$

The site balances are:

$$\begin{aligned}\theta_E+\theta_{EH_2}+\theta_{EH_4}+\theta_S&=1 \qquad \text{non-competitive adsorption}\\ \theta_H+\theta_*&=1\end{aligned} \tag{14}$$

$$\theta_H+X\theta_E+X\theta_{EH_2}+X\theta_{EH_4}+\theta_*=1 \quad \text{competitive adsorption} \tag{15}$$

It should be noted that the site balance for the competitive case has to be solved iteratively unless $X=1$. Elimination of the surface coverages $\theta_E...\theta_{EH_4}$ results in the final rate equations:

non-competitive adsorption

$$r=\frac{k_3\frac{k_1}{k_{-1}}\frac{k_2}{k_{-2}}K_E K_H^3 p_E p_H^3}{(a'K_E p_E+1)(K_H^{1/j}p_H^{1/j}+1)^j\left(1+\frac{k_3}{k_{-2}}(K_H p_H)+\frac{k_2k_3}{k_{-1}k_{-2}}(K_H p_H)^2\right)} \tag{16}$$

competitive adsorption $(X=1)$

$$r=\frac{k_3\frac{k_1}{k_{-1}}\frac{k_2}{k_{-2}}K_E K_H^3 p_E p_H^3}{(a'K_E p_E+K_H^{1/j}p_H^{1/j}+1)^{j+1}\left(1+\frac{k_3}{k_{-2}}(K_H p_H)+\frac{k_2k_3}{k_{-1}k_{-2}}(K_H p_H)^2\right)} \tag{17}$$

where a′ is given by:

$$a'=\frac{1+\left(\frac{k_1}{k_{-1}}+\frac{k_3}{k_{-2}}\right)K_H p_H+\left(\frac{k_1}{k_{-1}}\frac{k_2}{k_{-2}}+\frac{k_1}{k_{-1}}\frac{k_3}{k_{-2}}+\frac{k_2}{k_{-1}}\frac{k_3}{k_{-2}}\right)K_H^2 p_H^2}{1+\frac{k_3}{k_{-2}}(K_H p_H)+\frac{k_2k_3}{k_{-1}k_{-2}}(K_H p_H)^2} \tag{18}$$

The Marquardt–Levenberg parameter estimation method implemented in MAINA Non-linear Regression Package [18] was used to minimize the residual sum of squares between experimental and calculated reaction rates for the entire temperature range simultaneously. To reduce the amount of parameters the adsorbed hydrogen was presumed to be immobile compared to gas-phase hydrogen. Thus the hydrogen adsorption entropy was fixed to the negative value of the hydrogen absolute entropy in the gas phase at the temperatures used in the experi-

Table 3
Kinetic parameters (95% confidence), residual sum of squares (*SSQ*, arb. units) and mean residual sum of squares (*MRSQ*, arb. units) for the mechanistic reaction rate models, $k_i = [\,] \cdot 10^{-4}$ mol $s^{-1}$ $g_{Ni}^{-1}$, $E_i = [\,] \cdot$ kJ $mol^{-1}$, $\Delta S_i = [\,] \cdot$ J $mol^{-1}$ $K^{-1}$, $\Delta H_i = [\,] \cdot$ kJ $mol^{-1}$

| | Non-competitive adsorption | | Competitive adsorption | |
|---|---|---|---|---|
| | dissociative hydr. ads., Model I | non-dissoc. hydr. ads., Model II | dissociative hydr. ads., Model III | non-dissoc. hydr. ads., Model IV |
| *Equal rate constants* | | | | |
| *MRSQ* | 0.24 | 0.20 | 0.24 | 0.21 |
| *SSQ* | 14.9 | 12.8 | 14.6 | 13.3 |
| $k(\bar{T})$ | 334 ± 124 | 229 ± 94 | 1354 ± 127 | 734[a] |
| $-E$ | 100 ± 6 | 111 ± 4 | 102 ± 4 | 106[a] |
| $k_-(\bar{T})$ | 41.7 ± 15.0 | 17.3 ± 5.2 | 354 ± 33 | 75.2[a] |
| $-E_-$ | 91.9 ± 11.3 | 113 ± 9 | 99.5 ± 8.1 | 99.6[a] |
| $X$ | – | – | 4.6 ± 2.0 | 5.4[a] |
| $-\Delta S_H$ | 140 ± 0.3 | 140 ± 0.3 | 140 ± 0.3 | 140[a] |
| $-\Delta H_H$ | 53.9 ± 1.8 | 53.0 ± 1.7 | 56.3 ± 0.3 | 53.9[a] |
| $-\Delta S_E$ | 100 ± 5 | 111 ± 2 | 128 ± 3 | 180[a] |
| $-\Delta H_E$ | 54.7 ± 2.4 | 59.5 ± 24.9 | 66.5 ± 1.2 | 88.0[a] |
| | Non-competitive adsorption | | Competitive adsorption | |
| | dissociative hydr. ads. Model V | non-dissoc. hydr. ads. Model VI | dissociative hydr. ads. Model VII | non-dissoc. hydr. ads. Model VIII |
| *Uncoupled rate constants* | | | | |
| *MRSQ* | 0.17 | 0.18 | 0.24 | 0.21 |
| *SSQ* | 9.6 | 10.4 | 13.3 | 11.7 |
| $k_1(\bar{T})$ | 594 ± 405 | 176 ± 87 | 2496[a] | 1026[a] |
| $-E_1$ | 91.4 ± 70.7 | 78.6 ± 37.1 | 90.4[a] | 100[a] |
| $k_{-1}(\bar{T})$ | 86.3 ± 77.5 | 5.8 ± 5.1 | 945[a] | 95.8[a] |
| $-E_{-1}$ | 69.4 ± 64.4 | 76.1 ± 57.8 | 105[a] | 110[a] |
| $k_2(\bar{T})$ | 450 ± 18 | 289 ± 27 | 1750[a] | 650[a] |
| $-E_2$ | 135 ± 32 | 129 ± 97 | 136[a] | 126[a] |
| $k_{-2}(\bar{T})$ | 18.8 ± 8.8 | 44.7 ± 46.5 | 185[a] | 42.0[a] |
| $-E_{-2}$ | 99.7 ± 55.0 | 153 ± 44 | 91.3[a] | 87.3[a] |
| $k_3(\bar{T})$ | 163 ± 152 | 247 ± 287 | 790[a] | 494[a] |
| $-E_3$ | 50.9 ± 29.2 | 123 ± 106 | 73.6[a] | 79.9[a] |
| $X$ | – | – | 4.7[a] | 5.5[a] |
| $-\Delta S_H$ | 140 ± 0.2 | 140 ± 0.3 | 140[a] | 140[a] |
| $-\Delta H_H$ | 53.7 ± 0.1 | 53.0 ± 1.8 | 56.3[a] | 53.9[a] |
| $-\Delta S_E$ | 104 ± 4 | 107 ± 0.1 | 126[a] | 180[a] |
| $-\Delta H_E$ | 56.9 ± 1.8 | 58.0 ± 0.2 | 65.7[a] | 88.2[a] |

[a] 95% confidence intervals could not be calculated due to coupling between the parameters.

ments ($\Delta S_H = -140$ J $mol^{-1}$ $K^{-1}$). The possibility of all surface rate constants being equal ($k_1 = k_2 = k_3$ and $k_{-1} = k_{-2} = k_{-3}$) was tested first and compared to the case with uncoupled surface rate constants. The calculated kinetic parameters, as well as the residual sum of squares (*SSQ*) and mean residual sum of squares (*MRSQ*), for all eight modifications of the mechanistic model are given in Table 3.

All models were able to describe the experimental data with approximately equal and acceptable mean residuals, although the models featuring non-competitive adsorption and uncoupled rate constants seem to give a slightly better description according to the *MRSQ* values. Comparison of the calculated confidence intervals given in Table 3 reveal no great difference between the models, except that for three of the models with competitive adsorption no confidence intervals could be calculated due to strong coupling between the model parameters. The confidence intervals for the other models do generally not exceed 5% of the parameter values for the adsorption parameters. For the activation energies and rate constants, however, coupling between the constants are seen as large confidence intervals, especially for the cases with uncoupled rate constants as expected.

A better criterion for model comparison is the physical reasonability of the calculated parameters. Although the cases with equal rate constants are chemically improbable, no great improvement was achieved in the sum of squares nor in the distribution of the residuals by decoupling the rate constants from each other. The results for the model with equal rate constants, non-competitive adsorption and dissociative hydrogen adsorption (Model I) is illustrated in Fig. 6a as an example of the fit with equal rate constants. Fig. 7a illustrates that the corresponding case with decoupled rate constants (Model V) gives just a slightly better quality of description. Both cases show an approximately even distribution of the residuals as function of temperature (Figs. 6b and 7b, respectively) and reactant pressures.

An attempt to discriminate between the four models with decoupled surface rate constants led us to prefer the models with non-competitive adsorption (models V and VI) over the models with competitive adsorption (models VII and VIII). Model VII (dissociative hydrogen adsorption) shows a slightly temperature-dependent residual distribution (Fig 8b), although the overall fit was acceptable (Fig. 8a) also in this case. Model VIII (non-dissociative hydrogen adsorption) gave the value $-88.2$ kJ mol$^{-1}$ for the aromatic adsorption enthalpy, which appears to be too high according to calorimetrically measured heats of adsorption [19] for benzene on nickel at medium coverages (40–60 kJ mol$^{-1}$). However, the cases with competitive and non-competitive adsorption are of course extreme ones and the true nature of the coadsorption of these molecules lies somewhere in between these extreme cases. It would be expected that some competition takes place, since both components adsorb on the metal. Mirodatos [20] showed, however, by $H_2$–$D_2$ titration that the amount of adsorbed deuterium is not much different in the presence and in the absence of benzene on nickel. Also, the size of the aromatic molecules does not possibly allow them to rule out completely the much smaller hydrogen atoms or molecules from the surface.

The calculated adsorption parameters (model V and VI, Table 3) for ethylbenzene suggest that the adsorbed species is mobile on the surface ($\Delta S_E \approx -110$ J mol$^{-1}$ K$^{-1}$) and not very loosely bound ($\Delta H_E \approx -60$ kJ mol). Van Meerten and Coenen [2] suggest adsorption entropies of $-138$ J mol$^{-1}$ K$^{-1}$ for mobile adsorption of benzene on nickel, and calorimetric measurements reveal that the adsorption

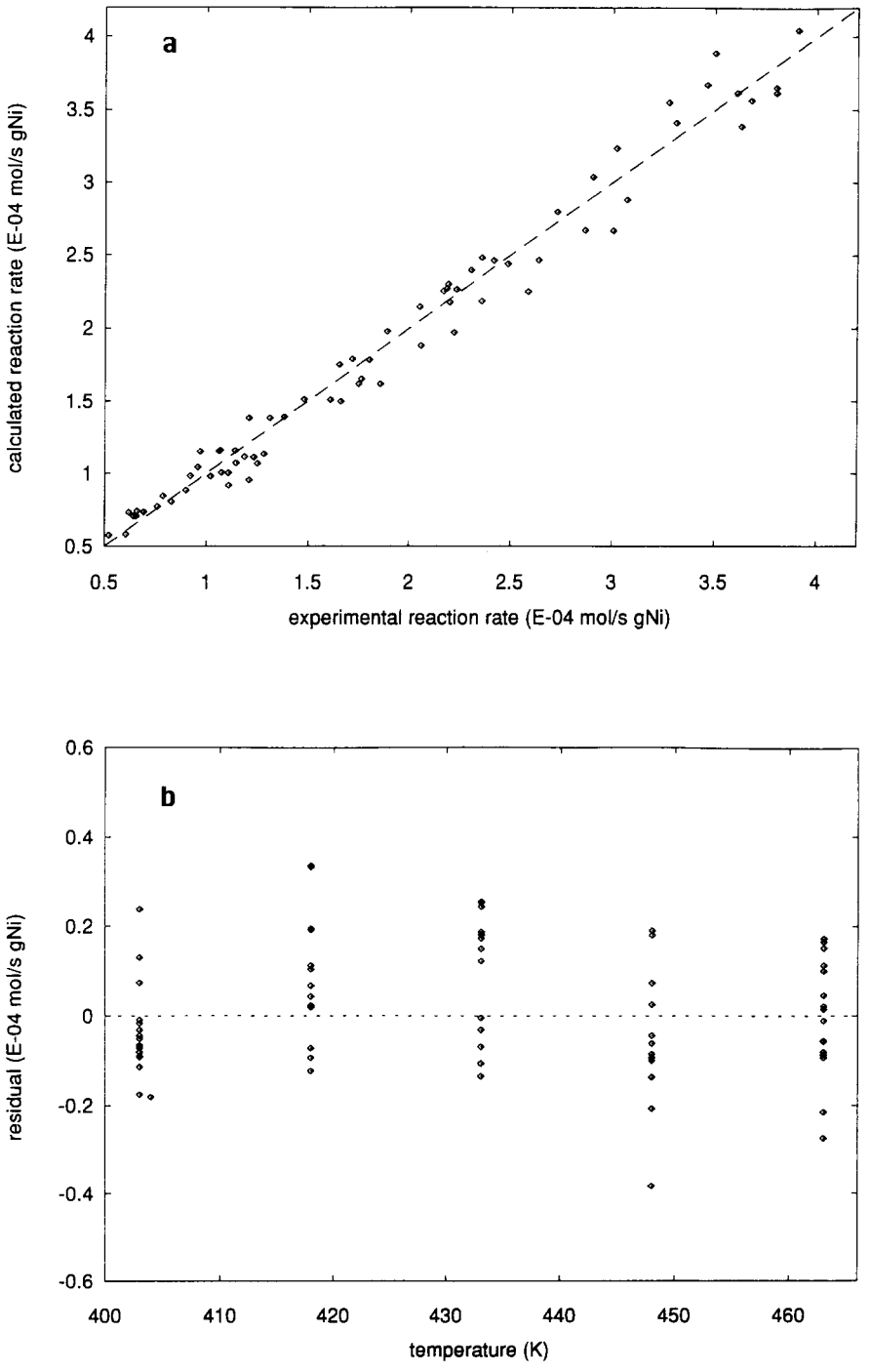


Fig. 6. Results of fit for model I (a): calculated versus experimental reaction rate (b): residuals as a function of temperature.

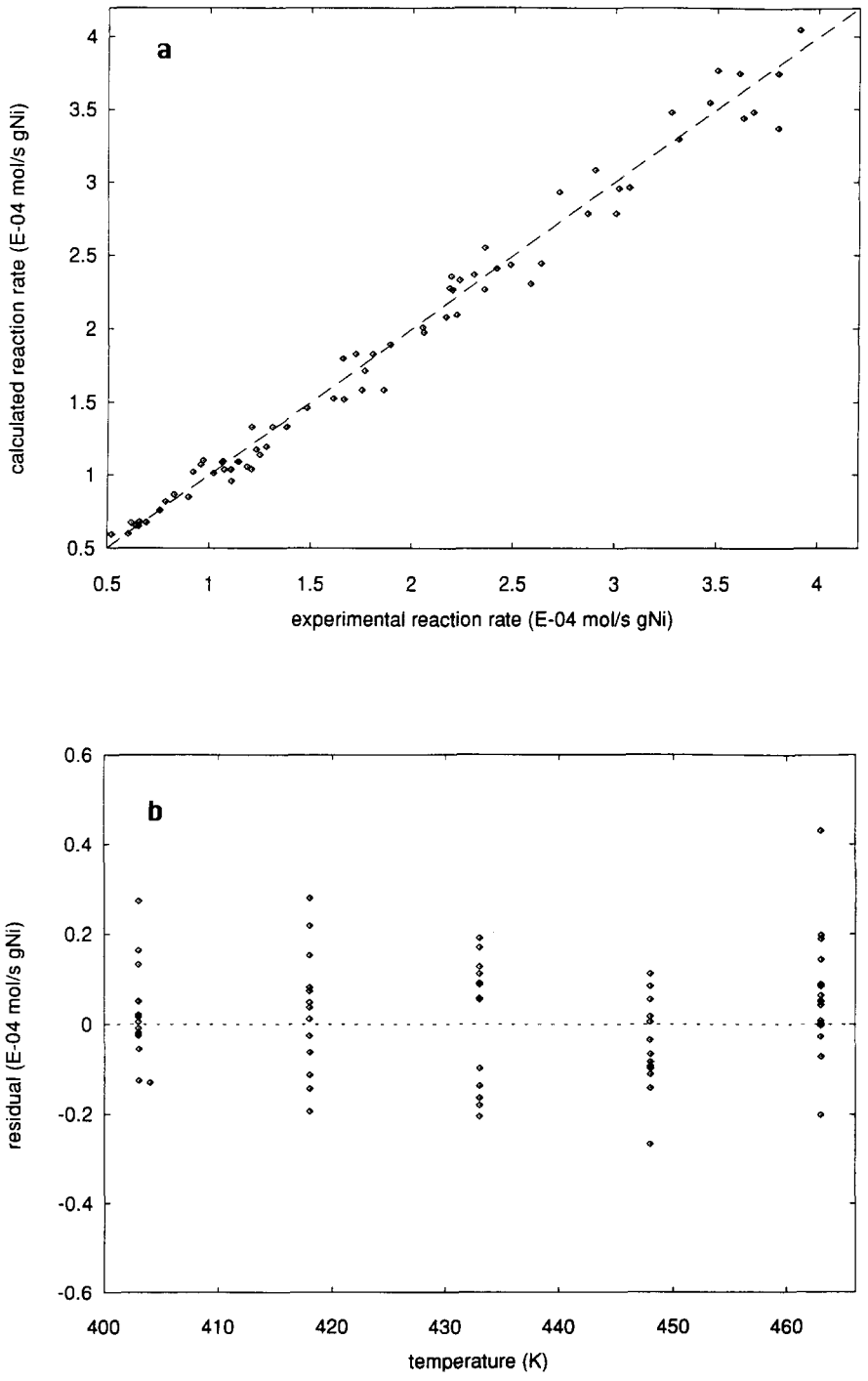


Fig. 7. Results of fit for model V (a): calculated versus experimental reaction rate (b): residuals as a function of temperature.

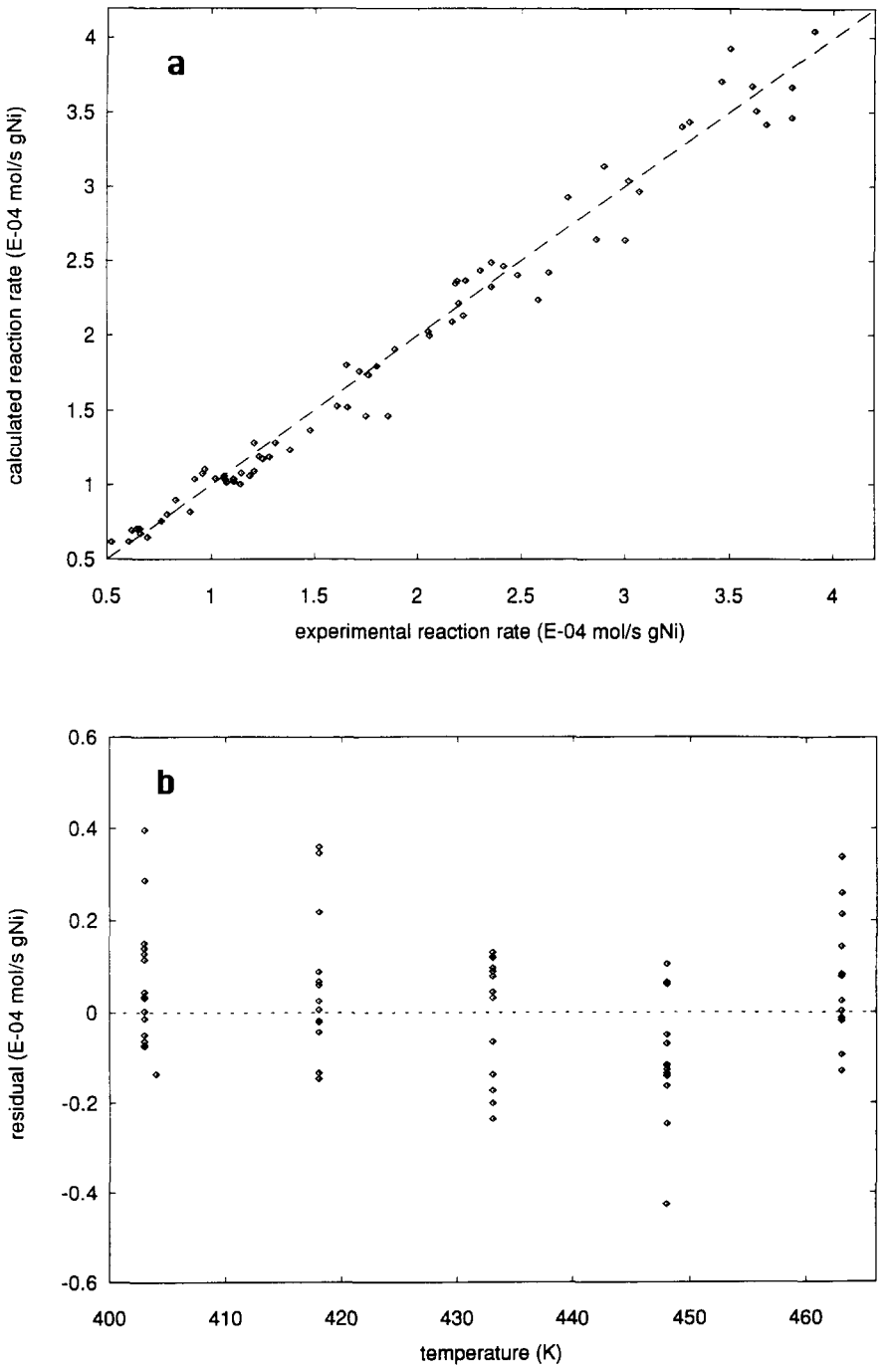


Fig. 8. Results of fit for model VII (a): calculated versus experimental reaction rate (b): residuals as a function of temperature.

enthalpy of benzene on nickel is 40–60 kJ $mol^{-1}$ at medium coverages [19]. The calculated adsorption enthalpy for hydrogen ($\Delta H_H \approx 53$ kJ $mol^{-1}$) is in good agreement with calorimetric chemisorption enthalpies measured at high surface coverages [21].

No discrimination based on our data could be made between dissociative hydrogen adsorption (model V) and non-dissociative hydrogen adsorption (model VI). Van Meerten et al. [22] used low-field magnetization measurements to show that the hydrogen active in hydrogenation of benzene on nickel is indeed dissociatively adsorbed. The fact that addition of two hydrogen atoms to the aromatic molecule is a three-body process can in our opinion not rule out the possibility of pairwise addition of hydrogen molecules, since the surface species are not expected to be nearly as mobile as in the fluid phase.

Sequential surface addition of hydrogen via the cyclohexadiene and cyclohexene intermediates is commonly proposed in the literature [2,3,13] as the mechanism of hydrogenation of aromatic compounds. We estimated the values of gas-phase equilibrium constants for hydrogenation reactions of ethylbenzene into ethylcyclohexadiene, ethylcyclohexene and ethylcyclohexane according to the Yoneda method [23]. The equilibrium constant of the former reaction is so small that reaction is almost impossible, the thermodynamical uphill in the formation of ethylcyclohexadiene being $\Delta G \approx 50$ kJ $mol^{-1}$. The reason lies in the loss of the resonance energy of the aromatic ring. Since we find no reason to assume very different adsorption behaviour of ethylbenzene compared to the hypothetical ethylcyclohexadiene intermediate, the thermodynamic constraints on this reaction path have to be accepted. This view is also supported by hydrogen reaction orders higher than two observed by other authors [9,13]. Reaction orders higher than one would have to involve the hypothetical ethylcyclohexadiene intermediate in the rate determining steps (in significant surface concentrations), which is not possible due to the low equilibrium constant already mentioned. The hydrogen reaction orders observed higher than two [9,13] would necessitate the involvement of the hypothetical ethylcyclohexene surface intermediate. In hydrogenation of cyclohexene, rates several orders of magnitude higher than for benzene have been observed [2,17,27]. Thus, ethylcyclohexene as such would not be present on the surface in significant amounts to take part in the rate limiting steps.

The aromatic molecule possibly forms intermediates with the added hydrogen atom pairs, still retaining the aromatic character and loosing the aromatic character after the third surface addition step [24,25]. The nature of the intermediate complexes on the surface of the catalyst can be considered using the 'aromaticity principle', which was proposed for the explanation of the Balandin's multiplet theory of heterogeneous catalysis [26]. According to this principle, in heterogeneous catalysis, the reaction occurs predominantly through intermediate compounds or transition states, in which the atoms of the reactants and the catalyst form rings with aromatic character. Thus the surface complex $EH_2S$ could be a doublet complex, where the added part contains two atoms of catalyst and two atoms of

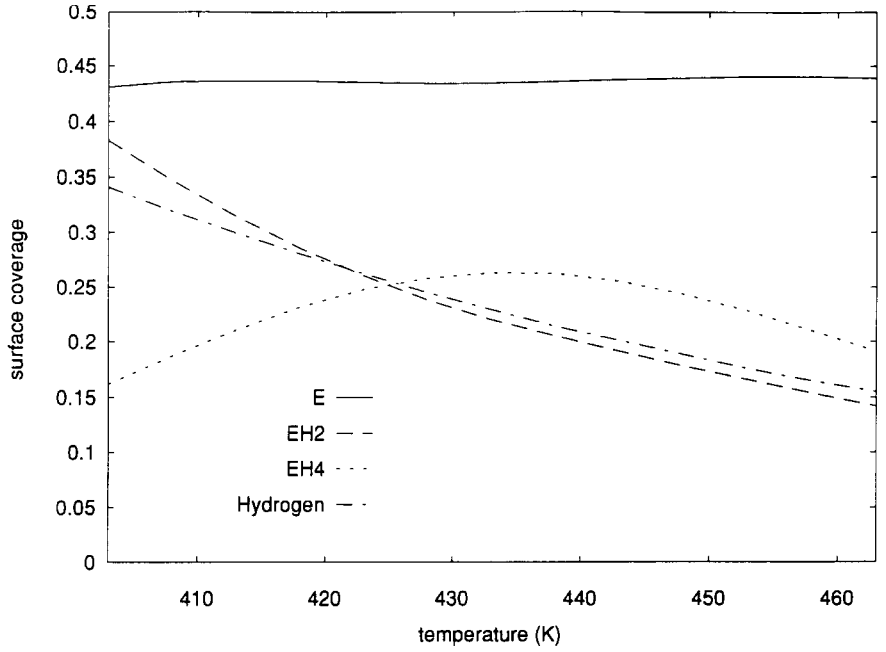


Fig. 9. Coverages of surface intermediates as a function of temperature according to model V.

hydrogen, resembling a naphthalene derivative. Such a complex is formed, without loosing the aromatic ring, with some additional resonance energy. The complex $EH_6S$ is consequently pictured as the aromatic molecule with three such 'added rings', all with aromatic character.

These considerations are also supported by the even distribution of surface coverages of the intermediates (ES, $EH_2S$ and $EH_4S$) calculated from model V (Fig. 9). All the other models predict approximately similar coverage distributions on the surface. An ethylcyclohexene surface intermediate would give us an essentially higher rate constant for the third addition step ($k_3$) and a negligible coverage of the $EH_4$ intermediate on the surface. It is also known that cyclohexenes are detected in the gas phase during hydrogenation of aromatic compounds. According to the view presented here, this could be the result of a parallel reaction path where the intermediate looses its aromatic character after the second hydrogen addition step [24].

## 4. Conclusions

The steady-state reaction rate of gas-phase hydrogenation of ethylbenzene on $Ni/Al_2O_3$ is strongly affected by reversible deactivation of the catalyst. Reactivation in flowing hydrogen at 400°C completely restores the initial activity of the catalyst. The deactivation behaviour may explain some of the disagreements in the literature

concerning the kinetics of hydrogenation of aromatic compounds, as often in kinetic modelling this deactivation process is not taken into account.

The calculated initial steady-state reaction rates, without the influence of deactivation, show a similar kinetic behaviour compared to the kinetics of hydrogenation of benzene and toluene over Group VIII metals. This implies a rate maximum as a function of temperature, near zero order towards the aromatic compound and positive reaction order towards hydrogen, the reaction orders increasing with temperature.

A mechanistic model featuring equilibrated adsorption steps, non-competitive adsorption, rate determining surface addition steps (pairwise addition) and fast desorption of the product, describe the data satisfactorily with physically reasonable parameters. The model suggests that the surface rate constants are not hugely different from each other and that the adsorption of the reactants is relatively weak in terms of adsorption energy.

Thermodynamic considerations, observed hydrogen reaction order ($>2$) and calculated surface rate constants led us to suggest that the surface intermediates retain their aromatic character through the hydrogen addition steps and loose the aromatic character after the last addition step.

Steady state experiments alone, accompanied by mechanistic modelling, cannot provide tools for a definite discrimination between rival mechanistic models with some common features. Therefore further studies, especially on the deactivation mechanisms, with transient and spectroscopic techniques are planned for the future.

## 5. Notation

| | |
|---|---|
| $a'$ | dimensionless constant, in Eqs. (16) and (17) |
| $a,b$ | empirical deactivation parameters, in Eq. (1) |
| $E$ | activation energy |
| $f$ | function, in Eq. (6) |
| $\Delta H$ | enthalpy of adsorption |
| $j$ | number of surface sites for hydrogen adsorption |
| $k$ | empirical rate constant, in Eq. (2) |
| $k_i$ | rate constant for step $i$ |
| $k'$ | lumped constant, in Eq. (6) |
| $K$ | adsorption equilibrium constant |
| $K_1,K_2$ | empirical equilibrium parameters, in Eq. (2) |
| $l,m,n$ | empirical exponents, in Eq. (2) |
| $p$ | partial pressure |
| $r$ | reaction rate |
| $R$ | gas constant |
| $r_0$ | initial reaction rate |
| $\Delta S$ | entropy of adsorption |

| | |
|---|---|
| $t$ | time |
| $T$ | temperature |
| $T'$ | transformed temperature |
| $\bar{T}$ | average temperature |
| $Y_i$ | lumped constant, in Eq. (6) |
| $X$ | number of surface sites occupied by aromatic compound |
| $\theta$ | fractional surface coverage |

*Subscripts and superscripts*

| | |
|---|---|
| $i$ | compound index |
| $S$ | vacant site for adsorption of an aromatic compound |
| $*$ | vacant site |

*Abbreviations*

| | |
|---|---|
| D | deuterium |
| E | ethylbenzene |
| ES | adsorbed ethylbenzene |
| $EH_2S$, $EH_4S$ | surface intermediates |
| $EH_6S$ | adsorbed ethylcyclohexane |
| EtCH | ethylcyclohexane |
| H | hydrogen |
| *SSQ* | residual sum of squares |
| *MRSQ* | mean residual sum of squares |

## Acknowledgements

The financial support from Neste Oy Foundation (S.S.) and Centre of International Mobility (D.M.) is gratefully acknowledged. The authors thank Mr. Markku Reunanen from the Laboratory of Forest Products Chemistry, Åbo Akademi, for assistance with the GC–MS analysis.

## References

[1] J. Völter, B. Lange and W. Kuhn, Z. Anorg. Allgem. Chem., 340 (1965) 253.
[2] R.Z.C. van Meerten and J.W.E. Coenen, J. Catal., 46 (1977) 13.
[3] Y.S. Snagovskii, G.D. Lyubarskii and G.M. Ostrovskii, Kinet. Katal., 7 (1966) 232.
[4] N.E. Zlotina and S.L. Kiperman, Kinet. Katal., 8 (1967) 1129.
[5] C. Mirodatos, J.A. Dalmon and G.A. Martin, J. Catal., 105 (1987) 405.
[6] J.P.G. Kehoe and J.B. Butt, J. Appl. Chem. Biotechnol., 22 (1972) 23.
[7] D. Klvana, J. Chaouki, D. Kusohorsky, C. Chavarie and G.M. Pajonk, Appl. Catal., 42 (1988) 121.
[8] L.M. Mamaladze, B.S. Gudkov and S.L. Kiperman, Izv. Akad. Nauk SSSR, Ser. Khim., 11 (1974) 2605.
[9] L.P. Lindfors and T. Salmi, Ind. Eng. Chem. Res., 32 (1993) 34.

[10] D.E. Mears, J. Catal., 20 (1971) 127.
[11] H.S. Fogler, Elements of Chemical Reaction Engineering, Prentice-Hall, Englewood Cliffs, NJ, 1986, p. 577.
[12] S.D. Lin and M.A. Vannice, J. Catal., 143 (1993) 563.
[13] P. Chou and M.A. Vannice, J. Catal., 107 (1987) 140.
[14] J.B. Butt and E.E. Petersen, Activation, Deactivation and Poisoning of Catalysts, Academic Press, San Diego, 1988, p. 49.
[15] S.L. Kiperman, Stud. Surf. Sci. Catal., 27 (1986) 3.
[16] L.M. Rose, Chemical Reactor Design in Practice, Elsevier, Amsterdam, 1981, p. 76.
[17] M. Boudart and C.M. McConica, J. Catal., 117 (1989) 33.
[18] B. Andersson, MAINA-Regression Program Package, Chalmers University of Technology, Gothenburg, 1994.
[19] Y-F. Yu, J.J. Chessick and A.C. Zettlemoyer, J. Phys. Chem., 63 (1959) 1626.
[20] C. Mirodatos, J. Phys. Chem., 90 (1986) 481.
[21] G. Wedler, Chemisorption: An Experimental Approach, Butterworths, London, 1976, p. 39.
[22] R.Z.C. van Meerten, T.F.M. de Graaf and J.W.E. Coenen, J. Catal., 46 (1977) 1.
[23] R.C. Reid, J.M. Prausnitz and B.E. Poling, Properties of Gases and Liquids, 4th ed., McGraw-Hill, Singapore, 1988, p. 157.
[24] M.I. Temkin, D. Yu. Murzin and N.V. Kul'kova, Dokl. Akad. Nauk SSSR, 303 (1988) 659.
[25] D. Yu. Murzin, N.A. Sokolova, N.V. Kul'kova and M.I. Temkin, Kinet. Katal., 30 (1989) 1352.
[26] M.I. Temkin, Kinet. Katal., 27 (1986) 533.
[27] G.A. Martin and J.A. Dalmon, J. Catal., 75 (1982) 233.